JOURNAL OF CATALYSIS 106, 47–53 (1987)

# Dispersed Cobalt-Containing Zeolite Fischer–Tropsch Catalysts

KERRY C. MCMAHON,* STEVEN L. SUIB,*,[1] BRYON G. JOHNSON,† AND CALVIN H. BARTHOLOMEW, JR.†,[1]

*Department of Chemistry and Institute of Materials Science, University of Connecticut, Storrs, Connecticut 06268, and †Department of Chemical Engineering, Brigham Young University, Provo, Utah 08402

Received July 1, 1986; revised February 16, 1987

Microwave discharge methods have been used to prepare highly dispersed cobalt clusters in zeolites. Ferromagnetic resonance, electron microscopy, and $H_2$ chemisorption experiments have been done to determine the particle sizes of the cobalt clusters. These materials were also studied as Fischer–Tropsch catalysts. Catalytic results suggest that these cobalt zeolite catalysts show high selectivity for the production of low-molecular-weight olefins. Evidence of shape selective catalysts with a cutoff at the $C_6$ chain length has also been observed. Our results are also in line with the concept of structure sensitivity. 

## INTRODUCTION

Recently, metal support interactions have been investigated in great detail (*1–5*). Adsorptive properties have been shown to be dependent on interactions between the metal and support (*1–5*). Activities and selectivities of supported metals in CO hydrogenation reactions have also attracted a great deal of attention.

Effects of metal dispersion on hydrocarbon selectivity have shown that the size of metal crystallites in catalysts can influence the size of hydrocarbons in Fischer–Tropsch syntheses (*6*). Specific activities for CO hydrogenation have been shown to decrease with increasing dispersion for cobalt (*7, 8*) and ruthenium catalysts (*9, 10*).

The effects of dispersion, extent of reduction, and catalyst preparation procedures for cobalt–alumina catalysts on the activity and selectivity in Fischer–Tropsch reactions have recently been summarized (*11*). Results of these studies indicate that CO hydrogenation on supported cobalt is a structure-sensitive reaction, that selectivity varies with metal loading, preparation, and pretreatment conditions (*11*).

We have recently reported (*12*) that highly dispersed cobalt catalysts can be prepared by a microwave discharge method. Synthetic conditions, characterization of the cobalt particles, and some of the reactions that occur in the discharge were studied. This paper deals with further characterization of cobalt-containing X zeolite catalysts by ferromagnetic resonance, scanning electron microscopy, energy dispersive X-ray analysis, and $H_2$ and $O_2$ chemisorption experiments. Particle sizes of the cobalt clusters were measured. Results concerning the activity and selectivity of these materials in Fischer–Tropsch reactions are also described here.

## EXPERIMENTAL

### *Synthesis of Catalyst*

A microwave discharge method (*12*) was used to prepare cobalt-containing zeolite X materials. An Ar gas pressure of 0.3 Torr and 1- to 3-W power were used in these experiments. The compound $Co_2(CO)_8$ was sublimed onto a dehydrated NaX zeolite. The plasma was ignited and the decomposition of the $Co_2(CO)_8$ occurred. After the reaction was complete, samples were sealed off, transferred to a dry box, and

[1] To whom correspondence should be addressed.



0021-9517/87 $3.00

loaded into cells for catalytic work and for ferromagnetic resonance studies. The completed CoNaX catalyst had a weight loading of 0.8% cobalt. Further details concerning the synthesis of these catalysts can be found elsewhere (*12, 13*).

### *Structural and Spectroscopic Characterization*

*Ferromagnetic resonance (FMR) experiments.* Ferromagnetic resonance (FMR) studies were done with either a Varian E-3 or E-9 spectrometer. An X-band microwave frequency of about 9.5 GHz was used in all experiments. Diphenylpicrylhydrazine (DPPH) was used as a calibration standard to determine $g$ values. All FMR experiments were done between temperatures of $-160$ and 285°C.

*X-ray powder diffraction.* X-ray powder diffraction experiments were done on a DIANO-XRD 8000 diffractometer. All experiments were done with copper $K_\alpha$ radiation. Samples were mounted on glass slides which had a slight coating of petroleum jelly. All scans were done at a rate of 2° $2\theta$/min.

*Scanning electron microscopy.* Scanning electron microscopy (SEM) was used to determine particle sizes of cobalt. Magnifications up to 98,000 × were done on an AMRAY 1000 SEM with an energy dispersive X-ray analysis (EDA × 9100/60) system.

### *Catalysis Experiments*

About 0.5 g of CoNaX zeolite was loaded into a quartz catalytic reactor in a $N_2$-filled dry box. The CoNaX sample was previously subjected to the microwave discharge procedure described earlier.

Experiments reported here were done between 1 and 3% conversion. Reaction temperature was between 512 and 544 K, and pressures of 1.00 atm were used. At least 17 runs were done on this material for a period up to 45 h. The $H_2$/CO ratio was 3.0. The space velocities at STP ranged from 390 to 680 per hour. The mass flow rate of reactants was $3.5–5.9 \times 10^{-3}$ g/min and the average molecular weight of the feed was 8.514 g/g-mol. These data are needed in order to reproduce flow rates. Further details concerning the synthesis of these catalysts can be found elsewhere (*12, 13*).

### *Hydrogen Chemisorption Measurements*

$H_2$ chemisorption measurements were performed in a conventional Pyrex glass, high-vacuum, volumetric adsorption apparatus. After reduction at 300°C, the catalyst was evacuated for 1 h to $2 \times 10^{-5}$ Torr at 290°C. $H_2$ was allowed to adsorb on the catalyst as it cooled from the evacuation temperature to room temperature over a period of 90 to 120 min at 400 Torr. Adsorption isotherms were then measured by a desorption (decreasing pressure) method (*7, 8, 11*). The straight-line portion of the isotherms were extrapolated to zero pressure to obtain the total gas uptakes.

## RESULTS

### *Ferromagnetic Resonance*

Ferromagnetic resonance spectra for CoNaX are shown in Fig. 1. The apparent $g$ value for this sample at $-160$°C is 2.35 while the value at room temperature is 2.18. A plot of the apparent $g$ value vs temperature is given in Fig. 2. The results indicate that a value of 2.18 is maintained from room temperature up to 160°C. By studying the linewidths of these samples as a function of

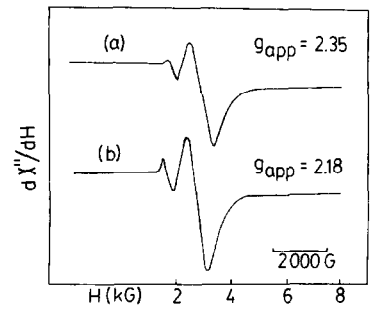


FIG. 1. Ferromagnetic resonance spectra of microwave activated CoNaX zeolite at (a) 113 K, (b) 298 K.

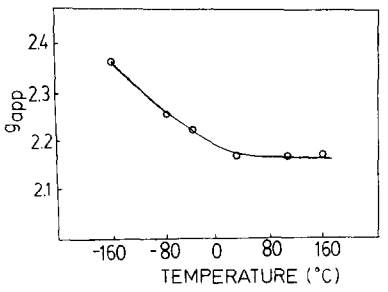


FIG. 2. Plot of apparent $g$ value vs temperature for superparamagnetic cobalt particles in NaX zeolite.

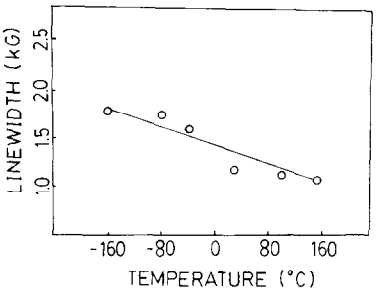


FIG. 3. Plot of ferromagnetic resonance linewidths (kG) vs temperatures.

temperature a linear plot, as shown in Fig. 3, is obtained. Smaller linewidths are observed at higher temperatures. These kinds of relationships are also observed for Co-NaY zeolites that have been prepared by microwave procedures (*12, 13*).

*Scanning Electron Microscopy*

Results of scanning electron microscopy studies of the CoNaX sample which had been passivated in air (*vide infra*) are given in Fig. 4. Figure 4a is an SEM photo of the CoNaX zeolite at low magnification. At higher magnification the photograph of Fig. 4b is obtained. This photograph shows that the surface of these particles is relatively featureless. A dot pattern for cobalt is given in Fig. 4c for the same area shown in Fig. 4b. The dots represent areas of high cobalt concentration.

*Catalytic Experiments*

Catalytic experiments were done for 48 h. Steady state conditions occur for these catalysts for hydrocarbons from $C_1$ through $C_{12}$.

Initial Fischer–Tropsch studies done at low (<1%) conversion (*14*) indicated that large amounts of olefins (mainly $C_2^{2-}$ and $C_3^{2-}$) as well as smaller amounts of saturated hydrocarbons (mainly $C_2$, $C_3$) were formed with CoNaX. A shape-selective effect was also observed with a cutoff at the $C_4$ chain length.

In the experiments described here, no alcohol products were detected. Both paraffins and olefin were formed ranging from $C_1$ through $C_9$. The activity/selectivity properties of the CoNaX sample are given in Table 1. Included in the table are the

TABLE 1

Activity/Selectivity Properties of Co/NaX (0.43 g)

| Temp (°K) | Time (h) | CO conversion (%) | $N_{CO} \times 10^3$ (molecules/site-s) | $CO_2$/HC (mol%) | Hydrocarbon product distribution (wt%) | | | | | O/P $C_3$–$C_7$ | $\alpha$ | $E_{act}$ (kJ/mole) |
|---|---|---|---|---|---|---|---|---|---|---|---|---|
| | | | | | $CH_4$ | $C_2$–$C_4$ | $C_5$–$C_{11}$ | $C_{12+}$ | Alcohols | | | |
| 512 | 2 | 1.42 | 0.37 | 16.3/83.7 | 28.5 | 45.4 | 26.1 | 0 | 0 | 1.17 | | 75 |
| 512 | 3 | 1.22 | 0.31 | 16.2/83.8 | 28.2 | 45.0 | 26.8 | 0 | 0 | 1.22 | | |
| 512 | 4 | 1.23 | 0.32 | 16.1/83.9 | 28.2 | 44.9 | 26.9 | 0 | 0 | 1.23 | | |
| 512 | 10.25 | 1.74 | 0.45 | 15.9/84.1 | 27.8 | 44.3 | 27.9 | 0 | 0 | 1.33 | 0.64 | |
| 512 | 16.5 | 1.01 | 0.26 | 15.7/84.3 | 27.4 | 43.5 | 29.1 | 0 | 0 | 1.37 | | |
| 512 | 19 | 1.81 | 0.47 | 16.2/83.8 | 28.3 | 43.8 | 27.9 | 0 | 0 | 1.39 | | |
| 522 | 20 | 1.72 | 0.59 | 18.3/81.7 | 32.7 | 42.3 | 25.0 | 0 | 0 | 1.41 | 0.61 | |
| 522 | 22.5 | 1.77 | 0.61 | 18.7/81.3 | 33.4 | 42.9 | 23.7 | 0 | 0 | 1.41 | | |
| 532 | 24.25 | 2.39 | 0.94 | 20.6/79.4 | 37.7 | 41.0 | 21.3 | 0 | 0 | 1.43 | 0.58 | |
| 532 | 26.5 | 2.08 | 0.82 | 21.1/78.9 | 38.6 | 41.0 | 20.4 | 0 | 0 | 1.44 | | |
| 544 | 33 | 2.41 | 1.09 | 23.5/76.5 | 44.3 | 38.6 | 17.1 | 0 | 0 | 1.45 | 0.54 | |
| 544 | 45 | 3.06 | 1.38 | 24.6/ | 46.9 | 38.0 | 15.1 | 0 | 0 | 1.49 | | |

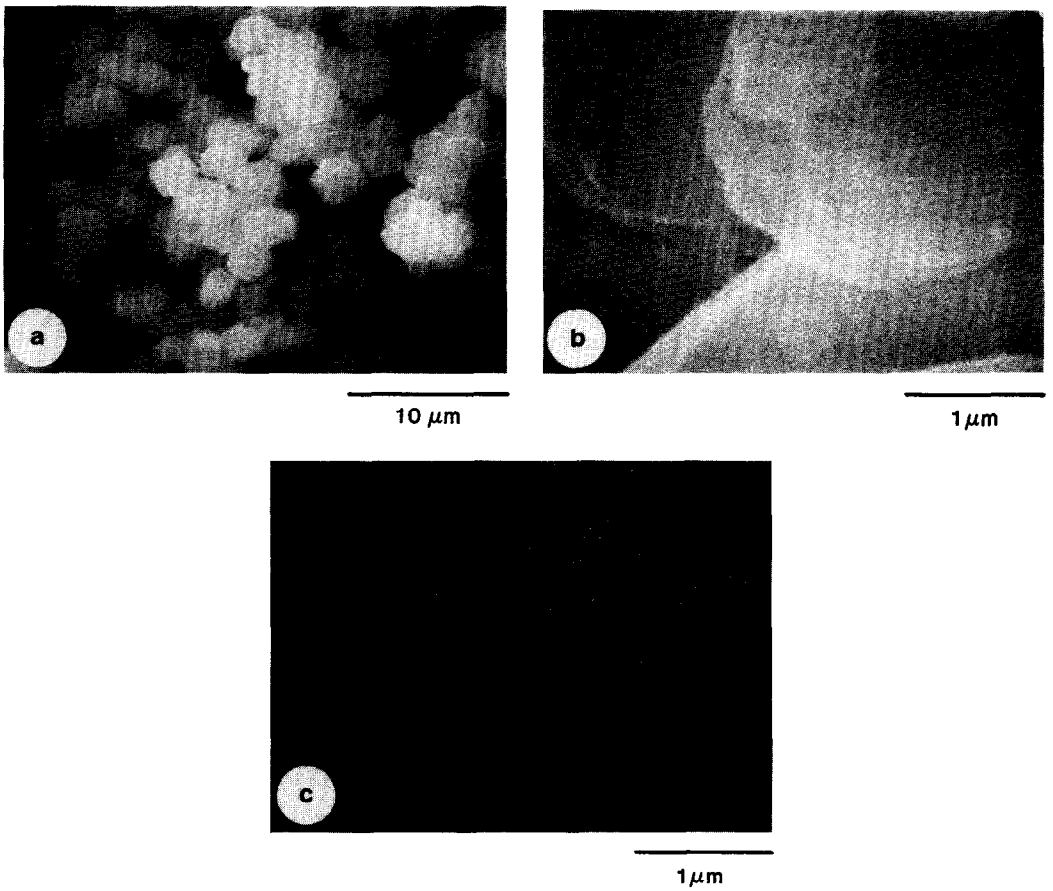


FIG. 4. Scanning electron micrographs of CoNaX zeolite passivated in dry $O_2$: (a) 3500× magnification, (b) 30,000× magnification, (c) energy dispersive X-ray analysis, cobalt dot pattern, same area as (b).

percent CO conversion, turnover frequencies, amount of $CO_2$ produced, hydrocarbon product distributions, olefin–paraffin ratios, parameters, and an activation energy.

Olefin-to-paraffin ratios for $C_2$–$C_7$ hydrocarbons are given in Table 2 for experiments done at temperatures between 512 and 544 K. An average weight percent of $C_2$–$C_4$ olefins in the total hydrocarbon product is given in Table 3.

An Anderson-Schulz-Flory plot for the CoNaX catalyst is given in Fig. 5. The corresponding plot of hydrocarbon

TABLE 2

Olefin/Paraffin Ratios of Co/NaX (Averages)

| $T$ (°K) | $C_2$ | $C_3$ | $C_4$ | $C_5$ | $C_6$ | $C_7$ |
|---|---|---|---|---|---|---|
| 512 | 1.16 | 6.86 | 0.49 | 0.76 | 0.51 | 0.23 |
| 522 | 0.95 | 6.50 | 0.54 | 0.91 | 0.49 | 0.23 |
| 532 | 0.77 | 5.85 | 0.56 | 0.83 | 0.50 | 0.22 |
| 544 | 0.75 | 5.47 | 0.51 | 0.74 | 0.50 | 0.20 |

TABLE 3

$C_2$–$C_4$ Olefins (wt%) (Average) in Hydrocarbon Product

| $T$ (°K) | $C_2$ | $C_3$ | $C_4$ | Total |
|---|---|---|---|---|
| 512 | 5.3 | 15.3 | 5.3 | 25.9 |
| 522 | 5.0 | 14.9 | 5.0 | 24.9 |
| 532 | 4.5 | 14.3 | 4.7 | 23.5 |
| 544 | 4.6 | 13.3 | 3.7 | 21.6 |

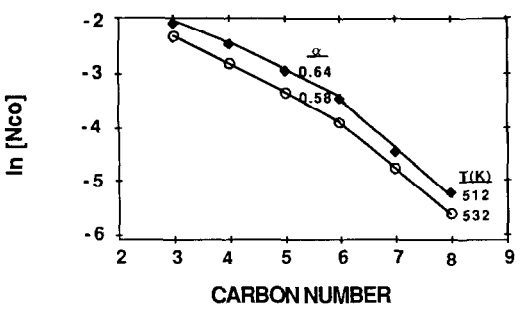


FIG. 5. Anderson–Schulz–Flory plot of hydrocarbon products from 0.8% Co/NaX ($H_2/CO$ = 3, 1 atm, and temperatures shown).

weight percent vs carbon number is given in Fig. 6.

### *Hydrogen Chemisorption*

The CoNaX catalyst had a $H_2$ adsorption uptake of 94 ± 5 μmol/g.

## DISCUSSION

### *Comparison of Microwave Discharge to Classical Reduction Methods*

It is useful to compare the microwave discharge method to more classical procedures for reducing metals. We (*15*) and others (*16–19*) have found it extremely difficult to prepare small iron clusters in zeolites. Thermal (*15*) and photochemical (*20*) procedures generally yield oxidized metal particles or larger (>30 Å) particles of the reduced metal on the external surface of the zeolite.

In the case of cobalt, Fraenkel and Gates (*21*) have used cadmium vapor to reduce $Co^{2+}$ ions in zeolite A. Ozin and co-workers (*22*) have used metal atom vaporization (low-temperature) methods to prepare highly reduced and dispersed cobalt clusters in the pores of zeolites. In general, however, thermal and photochemical methods lead to sintering of the metal (*15*). The catalytic properties of these systems will be discussed below.

We have measured the temperature of our microwave apparatus immediately after the microwave discharge and have found no increase in the *thermal* temperature of the reactor which is in contact with support. The *electronic* temperature, however, is undoubtedly much higher than room temperature. We cannot discount the effect of the light emission on the decomposition of the metal carbon bonds of the metal carbonyl although the intensity of this line emission is orders of magnitude lower than the intensity of a Xe photolamp.

### *Particle Size*

The FMR spectra of CoNaX in Fig. 1 clearly indicate that cobalt particles are extremely small and at least smaller than 30 Å. The fall in apparent $g$ value vs temperature of Fig. 2 and the decreasing linewidth as a function of temperature shown in Fig. 3 are also indicative of small ferromagnetic cobalt particles.

Scanning electron micrographs and energy dispersive X-ray analyses of CoNaX suggest that there are no large clusters (>100 Å) of cobalt in these materials. The EDX analysis confirms the presence of cobalt and that the cobalt is evenly dispersed throughout the sample.

X-ray line diffraction methods were used to try to examine the cobalt particles. No XRD peaks indicative of cobalt were observed. This observation suggests that the cobalt particles are less than about 40 Å.

The $H_2$ chemisorption uptake of 94 μmol/g is unexpectedly large for a catalyst containing only 0.8% Co. This uptake is comparable to those for Co–alumina (*8*)

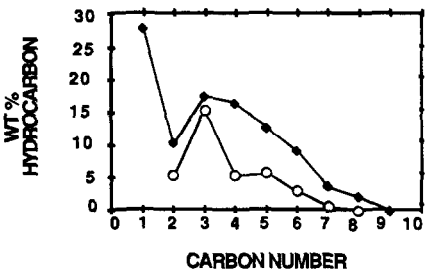


FIG. 6. Hydrocarbon product distribution from 0.8% Co/NaX at 512 K, 1 atm, $H_2/CO$ = 3. ■, total hydrocarbon product; ○, olefinic product.

and Co–silica catalysts (*11*) of conventional preparation having metal loadings in the range 15–25%. The large $H_2$ chemisorption uptake is indicative of very high (essentially 100%) dispersion and an average metal crystallite size of ≈9Å (*11*).

*Particle Location*

We have used Rutherford backscattering methods (*23*) to determine that the cobalt particles are distributed both on the surface and in the bulk of the X zeolite samples (*24*) prepared via the microwave deposition method.

*Catalysis Results*

*Activity*. The results of Table 1 indicate that low turnover frequencies ($\approx 0.3 \times 10^3$ molecules/site-s) at 512 K are observed. The range of turnover frequencies observed for this catalyst are about a factor of 10 lower than those observed for 3% Co on $Al_2O_3$ catalysts. These results suggest that these catalysts are not very active.

The observations of a decreased rate of methane production and a concomitant depression in overall rate has been observed for cobalt zeolite catalysts reduced by Cd vapor (*21*), cobalt on silicalite (*25*), and ruthenium Y zeolites (*26*). These studies (*21, 22, 25, 26*) and the present suggest that CO dissociation can be decreased with these materials resulting in lower yields of methane.

General agreement in the literature (*25*) is that at low conversions that CO dissociation is the limiting step.

*Selectivity*. There is a steady state for production of $C_1$–$C_{12}$ hydrocarbons for all experiments reported here.

The selectivities for $C_1$–$C_{11}$ hydrocarbons for the CoNaX catalyst are given in Table 1. The olefin to paraffin ratios for $C_3$–$C_7$ hydrocarbons also shown in Table 1 indicate a high selectivity toward olefins. The individual olefin/paraffin ratios of Table 2 show that there is an extremely large preference for propylene formation, and at 512 K for ethylene with respect to propane and ethane.

The data of Table 3 show that the weight percent olefin is larger at lower temperatures. A typical plot of hydrocarbon product vs carbon number is given in Fig. 6. The 26 wt% $C_2$–$C_4$ olefin in the total hydrocarbon product is larger than other cobalt zeolite catalysts (*21, 25*) although cobalt on silicalite shows a similar product distribution (*25*). The Anderson–Schultz–Flory plot of Fig. 5 shows a cutoff around $C_8$ which is in contrast to $CoAl_2O_3$ and Co–silicalite.

The values of chain growth propagation ($\alpha$) ranging from 0.54–0.64 are low relative to values of 0.7–0.9 observed for cobalt–alumina and cobalt–silica catalysts (*11*). However, this behavior is expected, since the catalyst in this study was tested at higher than normal reaction temperatures. The $\alpha$ values were calculated using only the linear portion of the Anderson–Schulz–Flory plots ($C_3$–$C_6$).

The tailoff in the ASF plots at the $C_6$–$C_9$ range is clear indication of a shape selective effect as a result of the zeolite support. The tailoff was observed at all reaction temperatures.

The activation energy of 75 kJ/mol for CoNaX is somewhat lower than observed for 3% Co/alumina (96 kJ/mol) prepared by conventional methods. But again, the higher temperature of reaction may contribute to a lower activation energy, involving, e.g., a different rate-determining step.

Another difference between the CoNaX zeolite and the Co–silicalite catalyst is that the largest chain observed with the silicalite catalyst is $C_{14}$. The CoNaX system has a cutoff at the $C_7$ chain length.

The high olefin yield, decreased methane yield, and large $CO_2$ by-product (16%) are indications that CO hydrogenation activity of Co on silicalite and NaX zeolite is low. This pronounced water–gas shift activity has been previously reported (*25*).

The results presented here suggest, then, that the Si/Al ratio, pore size of the zeolite, and/or the acidity of the support can drastically influence selectivity. Catalytic results for Co–A zeolites prepared by the

microwave method indicate larger amounts of methane (>50%) as well as for Co–ZSM-5 (*14*). The similarity of the Co–silicalite and CoNaX zeolite suggest that particle sizes and shapes may be similar but that electronic interactions of the cobalt with the support may influence selectivity.

A reviewer has suggested that instead of a shape-selective effect there may be a product holdup effect. We have tried to extract large-molecular-weight hydrocarbons to test for this but have not found them. In addition, the activity and selectivity of the catalyst are relatively constant suggesting there is no significant deactivation which would be expected if a product holdup effect was occurring.

Our data suggest that Co is better dispersed in X zeolite than in silicalite catalysts (*25*) which is manifested in a lower activation energy (75 kJ/mol) for systems reported here than the silicalite catalyst (*25*) (130 kJ/mol). The Co silicalite catalyst may make longer-chain hydrocarbons due to pore-size differences between the two catalysts.

## CONCLUSIONS

Our data indicate that CO hydrogenation on Co zeolite catalysts is a structure-sensitive reaction. These highly dispersed catalysts are not as active as catalysts with larger cobalt particles but show higher selectivities toward light hydrocarbons than cobalt–alumina catalysts. At 512 K the hydrocarbon product is 26% $C_2$–$C_4$ olefins. A tailoff in Anderson–Schultz–Flory plots at $C_6$–$C_9$ is indicative of a shape-selective effect. FMR, SEM, and $H_2$ chemisorption experiments indicate that the cobalt clusters are extremely small. $H_2$ chemisorption experiments indicate a 100% dispersion and a particle size of about 9 Å prior to catalytic experiments.

## ACKNOWLEDGMENT

K.C.M. and S.L.S. acknowledge the support of the Department of Energy, Office of Basic Energy Sciences for support of the work done at the University of Connecticut.

## REFERENCES

1. Jung, H. J., Walker, P. L., and Vannice, M. A., *J. Catal.* **75,** 416 (1982).
2. Tauster, S. J., and Fung, S. C., *J. Catal.* **55,** 29 (1978).
3. Tauster, S. J., Fung, S. C., and Garten, R. L., *J. Amer. Chem. Soc.* **100,** 170 (1978).
4. Vannice, M. A., and Garten, R. L., *J. Catal.* **56,** 236 (1979).
5. Zagli, A. E., Falconer, J. L., and Keenen, C. A., *J. Catal.* **56,** 453 (1979).
6. Nijs, M. M., and Jacobs, P. A., *J. Catal.* **65,** 328 (1980).
7. Reuel, R. C., and Bartholomew, C. H., *J. Catal.* **85,** 78 (1984).
8. Bartholomew, C. H., and Reuel, R. C., *Ind. Eng. Chem. Prod. Res. Dev.* **24,** 56 (1985).
9. Kellner, C. S., and Bell, A. T., *J. Catal.* **75,** 251 (1982).
10. Chen, Y. W., Wang, H. T., and Goodwin, J. G., *J. Catal.* **83,** 415 (1983).
11. Fu, L., and Bartholomew, C. H., *J. Catal.* **92,** 376 (1985).
12. Zerger, R. P., McMahon, K. C., Seltzer, M. D., Michel, R. G., and Suib, S. L., *J. Catal.* **99,** 498 (1986).
13. McMahon, K. C., Ph.D. Thesis, University of Connecticut, 1985.
14. (a) Suib, S. L., McMahon, K. C., and Zerger, R. P., Abstracts North Amer. Catal. Soc. Meeting, Houston, 1985, A-18; (b) see Ref. (*13*); (c) McMahon, K. C., and Suib, S. L., unpublished results.
15. Suib, S. L., McMahon, K. C., Tau, L. M., and Bennett, C. O., *J. Catal.* **89,** 20 (1984).
16. Morice, J. A., and Rees, L. V. C. *Trans. Faraday Soc.* **64,** 1388 (1968).
17. Delgass, W. N., Garten, R. L., and Boudart, M., *J. Phys. Chem.* **73,** 2970 (1969).
18. Lee, J. P., *J. Catal.* **68,** 27 (1981).
19. Huang, Y. Y., and Anderson, J. R., *J. Catal.* **40,** 143 (1975).
20. Nagy, J. B., Van Eenoo, M., and Derouane, E. G., *J. Catal.* **58,** 230 (1979).
21. Fraenkel, D., and Gates, B. C., *J. Amer. Chem. Soc.* **102,** 2478 (1980).
22. Nazar, L. F., Ozin, G. A., Hugues, F., Godber, J., and Rancourt, D., *Angew. Chem. Int. Ed. Engl.* **22,** 624 (1983).
23. Baumann, S., Strathman, M. D., and Suib, S. L., *J. Chem. Soc. Chem. Commun.*, 368 (1986).
24. Baumann, S., Strathman, M. D., Zhang, Z., and Suib, S. L., *Inorg. Chem.*, submitted.
25. Peuckert, M., and Linden, G., *in* "Proceedings, 8th International Congress on Catalysis, Berlin, 1984," Vol. 2, p. 135. Verlag Chemie, Basel, 1984.
26. Audier, M., Klinowski, J., and Benfield, E., *J. Chem. Soc. Chem. Commun.*, 626 (1984).